Infrared picosecond transient hole-burning studies of the effects of hydrogen bonds on the vibrational line shape

Infrared picosecond transient hole-burning studies of the effect of hydrogen bonds on the vibrational line shape

Mischa Bonn
FOM-Institute for Atomic and Molecular Physics, Kruislaan 407, 1098 SJ Amsterdam, The Netherlands and Schuit Institute of Catalysis, Eindhoven University of Technology, P.O. Box 513, 5600 MB Eindhoven, The Netherlands

Marco J. P. Brugmans[a] and Aart W. Kleyn
FOM-Institute for Atomic and Molecular Physics, Kruislaan 407, 1098 SJ Amsterdam, The Netherlands

Rutger A. van Santen
Schuit Institute of Catalysis, Eindhoven University of Technolgoy, P.O. Box 513, 5600 MB Eindhoven, The Netherlands

Huib J. Bakker
FOM-Institute for Atomic and Molecular Physics, Kruislaan 407, 1098 SJ Amsterdam, The Netherlands

(Received 11 March 1996; accepted 17 May 1996)

With infrared transient hole-burning spectroscopy we have investigated the influence of OD···X hydrogen bonds on the vibrational line shape of O–D stretch vibrations in acid zeolites. The effect of hydrogen bonding on the line shape depends critically on the type of hydrogen bond. For hydrogen bonding in a rigid structure, the hydrogen bond determines the *inhomogeneous* linewidth, but the *homogeneous* linewidth is determined by coupling to a $\sim$200 cm^{-1} lattice mode as concluded from the temperature dependence of the dephasing rate. When the hydrogen bond is formed with an adsorbing molecule, the coupling between the high-frequency O–D stretch vibration and the low-frequency OD···X hydrogen-bond stretching mode does determine the homogeneous linewidth. The difference between the two systems can be explained by the different hydrogen-bond potentials. Variation of the adsorbate provides a means of obtaining conclusive information on the coupling mechanism between the high-frequency O–D stretching mode and the low-frequency OD···X hydrogen-bond stretching mode. © *1996 American Institute of Physics.* [S0021-9606(96)02832-2]

I. INTRODUCTION

Infrared absorption line shapes have received considerable attention in the past decades, since it is clear that the center frequency and the width of an absorption line contain information on the interaction of a molecule or oscillator with its surroundings.[1] The effect of hydrogen bonds on the vibrational line shape is particularly interesting, since the bandwidth of a hydrogen-bonded complex is typically an order of magnitude larger than that of the free molecule. Although this problem has received considerable attention in both theoretical[2–7] and experimental[8–15] studies, there is substantial ambiguity as to the exact cause of this broadening and its appropriate theoretical description.

In this paper we investigate the effect of hydrogen bonding on the vibrational line shape of O–D stretch vibrations of deuterated hydroxyls in zeolites. Weak hydrogen bonds are formed by hydrogen bonding of the deuterated hydrogen atom of the hydroxyl group with zeolite lattice oxygen atoms, or by adsorption of simple molecules to available O–D sites in the zeolite. We have investigated the resulting absorption line with both conventional and time-resolved saturation IR spectroscopy. The latter technique allows us to separate homogeneous from inhomogeneous contributions to the line shape. It is found that the effect of the hydrogen bond on the homogeneous vibrational line shape depends strongly on the nature of the hydrogen bond: Absorption lines which are indistinguishable with conventional IR spectroscopy can hide very different homogeneous vibrational dynamics. The zeolite system allows us to ''tune'' the relevant physical parameters determining the absorption line, by choosing adsorbates with different masses and hydrogen-bond strengths. Thus we are able to obtain conclusive information on the coupling between the O–D stretch vibration and the OD···adsorbate hydrogen-bond stretching mode.

The O–D groups under investigation are the acid sites in the microporous alumino-silicate zeolites. These acid zeolites are used in solid acid catalyzed processes (e.g., hydrocarbon cracking in the petrochemical industry).[16] Insight in the dynamics of the microscopic interaction between the catalytic site and adsorbates is of essential interest for a fundamental understanding of zeolite catalysis and the theoretical description of these processes. The possible consequences of our findings for catalysis are discussed elsewhere.[17]

[a]Present address: The Netherlands Cancer Institute/Antoni van Leeuwenhoek Huis, Radiotherapy Department, Plesmanlaan 121, 1066 CX Amsterdam, The Netherlands.

II. THEORY

A. General linewidth theory

An absorption line can crudely be described in terms of inhomogeneous and homogeneous contributions. Inhomogeneous broadening is due to static structural properties of the sample. It occurs when different oscillators have slightly different transition frequencies due to the different environments they experience. Homogeneous broadening is connected to the twofold dynamics of the vibration: First, broadening will occur due to the finite lifetime of the excitation; population in the excited state will decay back to the ground state. The second cause for homogeneous line broadening is pure dephasing, due to the loss of coherence of the excitation. For a sub-ensemble of oscillators with the same center frequency, this means that the macroscopic polarization will decay in time, resulting in a line broadening, while the excitation itself need not decay. The lifetimes associated with the two decay mechanisms are the vibrational population lifetime T_1 and the pure dephasing time T_2^*, respectively. Homogeneous broadening will result in a line shape of width $2\pi\Gamma_{\mathrm{hom}}=T_1^{-1}+2T_2^{*-1}$.

A more precise theoretical description of the effect of pure dephasing on the absorption line involves *two* parameters which determine the absorption line: the width D of the spectral distribution determining the possible frequencies of the oscillators, and a correlation time τ_c, a measure of the time during which the oscillators retain the same frequency within the spectral distribution. In this description the frequency of an oscillator reads: $\tilde{\nu}(t)=\tilde{\nu}_0+\delta\tilde{\nu}(t)$,[2,3] with τ_c defined as the decay time of the time-correlation function of the oscillator detuning: $\langle\delta\tilde{\nu}(0)\delta\tilde{\nu}(t)\rangle\sim D^2e^{-t/\tau_c}$, and the frequency modulation is described as a Markovian process. If the spectral distribution is assumed to be Gaussian, the spectral line $A(\tilde{\nu})$ is determined by the decay of the polarization auto-correlation function $e^{-g(t)}$ as,[2,3]

$$A(\tilde{\nu})=\int_{-\infty}^{\infty}e^{i\tilde{\nu}t}\times e^{-g(t)}dt,$$

$$g(t)=D^2\tau_c^2[e^{(-t/\tau_c)}+t/\tau_c-1]. \tag{1}$$

In the so-called fast modulation limit ($D\tau_c\ll 1$), the exponential term in $g(t)$ is negligible, and $g(t)\approx D^2\tau_c t$. This results in a homogeneously broadened line with a Lorentzian shape of width $\sim D^2\tau_c$. Note that the faster the frequency modulation, i.e., the smaller τ_c, the narrower the absorption line: If the modulation of the transition frequency is sufficiently rapid, the net phase evolution of the oscillators resembles that of the central frequency of the distribution and the net phase difference between oscillators develops relatively slowly. As a result, the macroscopic polarization decays slowly, resulting in a sharp absorption band. This phenomenon is known in magnetic resonance spectroscopy as motional narrowing.[18]

In contrast, in the slow modulation limit ($D\tau_c\gg 1$), the exponential term in the expression of $g(t)$ can be expanded, and $g(t)\approx D^2t^2$. This results in an inhomogeneously broadened line: Due to the relatively slow modulation of the transition frequencies, the frequencies of the different oscillators are different and can be regarded as effectively fixed. In this limit, the line shape is determined *only* by D, the width of the spectral distribution, i.e., the range of possible transition frequencies. If there is a homogeneous broadening hidden in this inhomogeneous absorption band, these homogeneous absorption lines have to be described with a second combination of D' and τ_c'. In that case there are two mechanisms giving rise to a frequency modulation, one of which is slow (characterized by D and τ_c with $D\tau_c\gg 1$) and the other is fast (characterized by D' and τ_c' with $D'\tau_c'\lesssim 1$).

In the intermediate regime ($D\tau_c\approx 1$), a larger linewidth can be caused by either a slower modulation (larger τ_c) or a larger spectral distribution D. This intermediate regime is sometimes referred to as ''non-Markovian,'' since the collective decay of the macroscopic polarization of the ensemble of oscillators can no longer be described as a Markovian process.

Recent developments in time-resolved spectroscopic techniques have allowed for the separation of static and dynamic contributions to the vibrational linewidth. Homogeneous vibrational line shapes can be measured with IR transient hole-burning techniques[19,20] and recently the time-resolved observation of vibrational dephasing by means of an infrared photon-echo experiment was reported.[21]

Transient infrared hole-burning spectroscopy allows for the investigation of absorption lines by selectively exciting a sub-ensemble of oscillators within the overall absorption line. The presence of inhomogeneous broadening can be revealed, and the (quasi-)homogeneous linewidth, determined by the vibrational dynamics as well as the vibrational population lifetime T_1 can be obtained, providing us with the complete vibrational dynamics of the system.

B. Theoretical models for dephasing in hydrogen-bonded systems

A great number of sophisticated theoretical models have been developed to describe vibrational line shapes,[2–7,22,23] some specifically addressing the effect of hydrogen bonds.[5–7,22,23] Here, we will give a brief review of the relevant theories, the concomitant predictions and previous applications of these theories to explain the experimental observations.

In most of these theories the dephasing of the high-frequency $\overleftarrow{\mathrm{X}}$–$\overrightarrow{\mathrm{H}}\cdots\overleftarrow{\mathrm{Y}}$ ν_s stretching mode ($\sim$2600 cm^{-1} for our system) in the hydrogen-bonded X–H$\cdots$Y system is due to anharmonic coupling of this mode to the low-frequency ($\sim$100 cm^{-1}) $\overleftarrow{\mathrm{X}}$–$\overrightarrow{\mathrm{H}}\cdots\overleftarrow{\mathrm{Y}}$ ν_σ stretching mode. We will refer to the normal coordinates of the high-frequency ν_s and the low-frequency ν_σ stretching modes as r_s and r_σ, respectively. The two modes are expected to be strongly coupled since they lie along the same spatial coordinate and it has therefore been surmised that there is a strong correlation between the ν_s^{XH} frequency and the X$\cdots$Y hydrogen bond distance r_σ. The importance of the coupling of the two stretching motions for the infrared spectrum of the high-frequency ν_s mode was first pointed out by Marechal and Witkowsky.[5]

The key point of this theory was the recognition that the coordinate of the ν_σ(XH···Y) mode r_σ determines the frequency of the ν_s(X–H) mode. In this theory the relatively fast motion of coordinates r_s is separated from the slow motion in coordinates r_σ, in a vibrational Born–Oppenheimer approximation.[5] The result of this adiabatic description is a stick spectrum (absorption lines are delta functions) associated with the $v_{\mathrm{X-H}} = 0$ to $v_{X-H} = 1$ transition, made up of a vibrational progression in the ν_σ mode. The width of the overall absorption line is determined by how much the ν_σ mode can change its energy in going from $v_{\mathrm{X-H}} = 0$ to $v_{\mathrm{X-H}} = 1$. The theory was successfully employed to calculate infrared spectra for a single hydrogen-bonded complex; the agreement with experimental data for a gas-phase dimer and a hydrogen-bonded crystal was excellent.[5]

Bratos showed that in case of a hydrogen-bonded liquid it is not sufficient to consider a single hydrogen bonded complex.[6] In this model the description of the broad, featureless absorption spectrum presupposes a static distribution of hydrogen bond strengths, and a corresponding static distribution of transition frequencies. This means that this model describes broadening in the inhomogeneous limit of slow modulation ($D\tau_c \gg 1$).

In an extension of these static models by Robertson and Yarwood[7] the dynamics of the coupling were incorporated by introducing a stochastic modulation of the r_σ coordinate super-imposed on the ν_σ(XH···Y) vibration. This causes a frequency modulation of the high-frequency ν_s(X–H) mode through the time evolution of r_σ, which is described classically by means of a Langevin equation. The anharmonic coupling term V_{anh} describing the effect of the coupling of the ν_σ mode and the ν_s mode on the ν_s motion is *linear* in the coordinate $r_\sigma(t)$ of the ν_σ(XH···Y) mode in the spirit of Witkowski and Bratos: $V_{\mathrm{anh}} = K_{12} r_s^2 r_\sigma(t)$, with K_{12} the coupling constant. The result of this description is that, in case the ν_σ mode is overdamped (i.e., in the absence of combination bands between the ν_s and the ν_σ modes in the absorption spectrum), the width of the spectral distribution D is given by the coupling strength of the two modes and the root-mean-square amplitude of r_σ, $D = K_{12}\langle r_\sigma^2 \rangle^{1/2}$, and the correlation time τ_c is determined by a damping parameter γ for the ν_σ mode and the ν_σ frequency: $\tau_c = \gamma/\nu_\sigma^2$. The damping parameter γ reflects the damping of the hydrogen-bond mode ν_σ due to coupling of this mode to the bath.

This description is in sharp contrast with the theory of dephasing in condensed phases by Shelby and Harris,[4] in which the coupling depends linearly on the *occupation* of the low-frequency mode ν_σ, and hence the predominant coupling term depends on the coordinate r_σ to *second* order,[4] $V_{\mathrm{anh}} \propto r_\sigma^2(t)$. In this model, successfully applied to describe, amongst others, the homogeneous linewidth of a hydrogen-bonded polymer,[19] the modulation of the ν_s(X–H) transition frequency occurs through anharmonic coupling to the ν_σ low-frequency mode which undergoes energy exchange with the bath. Energy exchange between the low-frequency mode and the bath results in continuous excitation and de-excitation of the low-frequency mode. Since this mode is anharmonically coupled to the high-frequency mode, the transition frequency of the high-frequency mode is sensitive to whether or not the low-frequency mode is excited. Therefore energy exchange between the bath and the low-frequency mode will result in a modulation of the transition frequency of the high-frequency mode; the spectral distribution D is determined by the coupling strength and τ_c by the lifetime of the low-frequency mode, determined amongst others by the degree of thermal excitation of this mode. The key prediction of this theory is that, at low temperatures, the width of the absorption line will display an apparent activation energy with increasing temperature, equal to the energy of the low-frequency mode, due to the increased rate of thermal occupation of the low-frequency mode.[4]

Both the Robertson–Yarwood model and the Shelby–Harris model have been more or less successfully applied to describe line shapes in hydrogen-bonded systems.[15,19] However, from these and other experiments, it is clear that temperature variation,[12,19] change in hydrogen-bond strength by different hydrogen-bond acceptor/donor,[13] change of solvent[14] and isotopic substitution[15] lead to severe complications in the interpretation of the data, since too many parameters will change, affecting both D and τ_c that determine the line shape. Furthermore, considerable problems were encountered in background subtraction for the interpretation of the linear absorption spectra,[15] which has to be performed very accurately in order to obtain the true shape of the absorption band.

For strong hydrogen bonds in polar solvents, a direct dephasing mechanism has been proposed,[22–24] in which the ν_s(X–H) mode is coupled directly to the solvent, due to the dipolar interaction of the hydrogen-bonded group with the local solvent field. Although this description has successfully been applied to interpret experimental data (see, e.g., Ref. 24), we will not pursue this approach since in our systems with weak hydrogen bonds in rigid structures the hydrogen bond mode does play an important role in the dephasing process, as will be shown below. In this paper, we will compare the Shelby–Harris and the Robertson–Yarwood models in their ability to explain our experimental results.

III. EXPERIMENT

The zeolite samples consist of pressed self-supporting crystalline zeolite discs of ~ 5 mg/cm^2. Acid forms of Y-zeolite and Mordenite were obtained by *in vacuo* heating (1 h at 743 K) of the zeolite in which (part of the) Na^+ cations were exchanged by NH_4^+ cations. The two types of Y zeolite are specified by Si/Al ratios of 2.8 and H/T (T=Si or Al) ratios of 0.27 and 0.07, respectively. For the Mordenite the Si/Al and H/T ratios are 6.7 and 0.13 respectively. Deuteration is achieved by exposing the zeolite disc to 500 mbar of D_2 gas (Messer Griesheim, 99.7%) at 693 K and allowing exchange for 1 h, resulting in approximately 70% exchange as observed from the absorption spectra. These spectra were recorded using a Perkin–Elmer 881 double beam IR spectrometer. Adsorption of nitrogen (N_2, Messer Griesheim, 5.0), xenon (Xe, Messer Griesheim, 4.0), methane (CH_4,

L'Air Liquide, 3.5) and carbon monoxide (CO, Linde, 3.7) was performed at pressures ranging from 50 to 200 mbar, at temperatures from 100 to 170 K.

For the saturation experiments two independently tunable intense ($\approx 100\ \mu$J) picosecond (20 ps) infrared (2200–4500 cm^{-1}) pulses are generated by parametric downconversion of 1064 nm Nd-YAG pulses in $LiNbO_3$ crystals (an extensive description of the experimental setup can be found in Ref. 25). The pump repetition rate can be regulated from 1 to 10 shots per second, and was fixed at 5 Hz. At this repetition rate heating effects are negligible.[26] The pump energies were kept sufficiently low to justify the neglect of contributions from thermal desorption for the experiments on O–D groups with adsorbates. The laser pulse has a bandwidth of 6 cm^{-1} (FWHM, Gaussian line shape) at O–D absorption frequencies, which is four times smaller than the bandwidth at O–H frequencies. This better frequency resolution, and a reduced scattering of the laser pump light at O–D frequency as opposed to the O–H frequency, are the reasons for investigating the deuterated sample.

The setup allows for three kinds of experiments. The first type of experiment is a one-color pump–probe delay scan experiment. In this experiment the pump pulse is tuned to the O–D absorption frequency and focused onto the sample (focused beam ≈ 0.4 mm diameter). As a result, a considerable fraction ($\approx 20\%$) of the O–D oscillators are excited from their $v=0$ to $v=1$ vibrational state. Due to large anharmonicity (the O–D $v=1\rightarrow 2$ absorption is redshifted by ~ 100 cm^{-1} from the $v=0\rightarrow 1$ absorption) the excited O–D($v=1$) cannot absorb light at this frequency. This results in a bleaching of the O–D absorption on a picosecond time scale, i.e., a temporary increase of transmission of light at this wavelength through the sample. The subsequent equilibration of the population distribution can therefore be monitored by measuring the transmission of a weak probe pulse (of the same color) whose time delay with respect to the pump pulse can be varied. The decay of the pump-induced transmission with time is related to the vibrational lifetime of the excitation T_1, as: $\ln[T(t)/T_0] \sim \exp(-t/T_1)$, where $T(t)$ is the transmitted energy of the probe pulse at delay t and T_0 is the transmitted probe energy in absence of the pump pulse. Thus the vibrational lifetime of the first excited state can be obtained. It has been illustrated that monitoring the population difference between the ground and first excited state indeed renders the lifetime in the first excited state: No intermediate levels play a role in the decay process.[25]

The second type of experiment is a two-color frequency-scan experiment. In this experiment transient absorption spectra are recorded. The pump pulse is tuned to the $0\rightarrow 1$ transition, the delay between the pump and probe pulse is fixed, and the wavelength of the probe is scanned. Thus the spectral effect of the pump pulse can be investigated. This effect is twofold: After the pump pulse has excited the oscillators to their first excited state, the $0\rightarrow 1$ transition is bleached, resulting in an increased transmission at this frequency, but simultaneously absorption from $v=1$ to $v=2$ becomes possible. This transient, excited-state absorption band, shifted to lower frequencies compared to the $0\rightarrow 1$ transition due to the anharmonicity of the vibration, is called the hot band. From the width of the spectral hole that is burnt in the $0\rightarrow 1$ absorption band we can deduce the homogeneous linewidth for the $0\rightarrow 1$ transition. Analogously, the width of the $1\rightarrow 2$ transition (hot band) contains information on the vibrational dynamics of the $1\rightarrow 2$ transition.

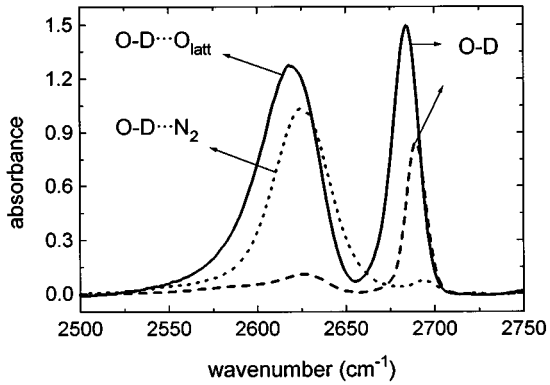

FIG. 1. Conventional absorption spectra for two of the deuterated zeolites under investigation, $D_{0.19}Y$ (solid) and $NaD_{.05}Y$ (dashed), and the spectrum for the latter with adsorbed nitrogen (dotted) in the O–D stretching region. Note the similarity between the vacuum LF O–D absorption band for $D_{0.19}Y$ (hydrogen bonded to the zeolite lattice) and the HF O–D···N_2 (hydrogen bonded to nitrogen) of the $NaD_{.05}Y$ zeolite.

In the third type of experiment, a two-color, 3-pulse, pump–pump–probe experiment, the first pump pulse is tuned to the $0\rightarrow 1$ transition, followed promptly by a second pump pulse tuned to the $1\rightarrow 2$ transition (slightly to the red). With this scheme approximately 5% of the oscillators can be excited to the second excited state $v=2$. With the probe pulse the population difference between the ground and first excited state, or between the first and the second excited state can be monitored as a function of delay between the pump pair and the probe. With this experiment, the lifetime of the *second* excited state can be obtained, as well as information on the decay route from $v=2$ down to $v=0$ (directly, or *via* $v=1$).

IV. RESULTS AND DISCUSSION

A. Differences between a solid and a gas-phase hydrogen bond

In Fig. 1 three absorption spectra in the O–D stretching region are shown. For $D_{0.19}Y$ zeolite (36 O–D groups per $Al_{52}Si_{140}O_{384}$ unit cell), two absorption peaks appear, one around 2680 cm^{-1}, associated with high-frequency (HF) O–D groups situated in the so-called supercages, and one around 2620 cm^{-1} originating from the low-frequency (LF) sites in the smaller cages.[27] The redshift of the LF O–D peak is due to a hydrogen bond between the deuterons from the LF O–D groups to zeolite lattice oxygen atoms.[28] These O–D groups will be further referred to as OD···O_{latt} groups. For the same zeolite with a lower concentration of O–D groups, $NaD_{0.05}Y$ (10 O–D groups per unit cell), mainly HF O–D groups in the large cages are present. Upon addition of

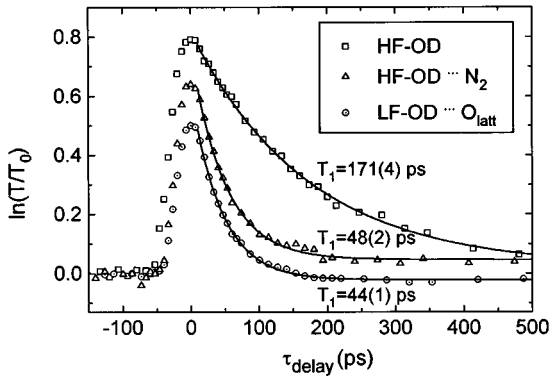

FIG. 2. Relative transmission of an infrared probe pulse $\ln[T(t)/T_0]$ (T_0 is the transmitted probe energy in absence of the pump pulse) as function of the delay between pump and probe pulses for three different hydroxyls: The ''free'' HF hydroxyls of $NaD_{0.05}Y$ in vacuum ($\square$), the same hydroxyls with nitrogen adsorbed ($\triangle$), $OD\cdots N_2$, and the LF hydroxyls of $D_{0.19}Y$ ($\odot$), $OD\cdots O_{latt}$, hydrogen bonded to the zeolite lattice. Note that the population-lifetimes for the latter two are practically equal. The values for the fitted population lifetimes T_1 (and the corresponding standard deviations) are denoted in the graph.

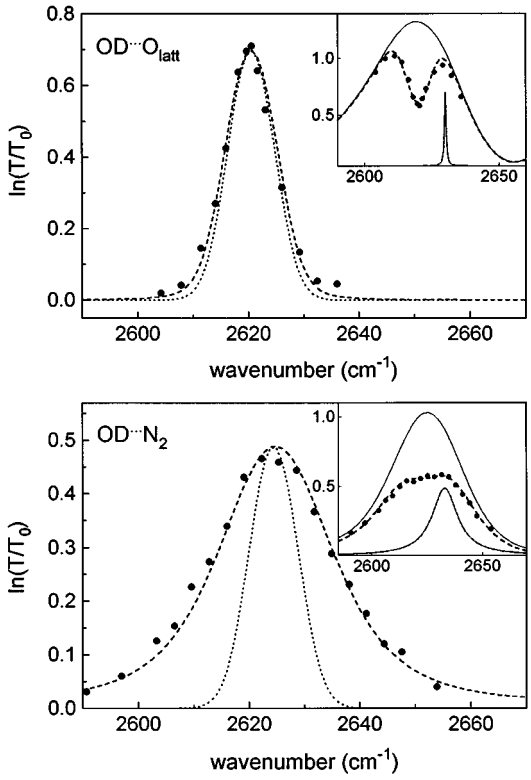

FIG. 3. Relative transmission changes due to the pump pulse tuned to the peak of the absorption band as a function of probe frequency, at 20 ps delay between pump and probe. Full circles are data, the dotted line is the instrumental function (convolution of the 6 cm^{-1} laser pump and probe pulses, viz. the observed signal for $\Gamma_{hom}\rightarrow 0$). Upper panel: The $OD\cdots O_{latt}$ hydroxyls of $D_{0.19}Y$ at 100 K. The width of the burnt hole is almost completely determined by the 6 cm^{-1} width of the laser pulses. Lower panel: The $OD\cdots N_2$ of $NaD_{0.05}Y$ at 100 K. Virtually the whole absorption band is bleached. Dashed lines are the result of calculations described in the text. Insets show the absorption spectra from Fig. 1 with (dashed curve) and without (solid curve) the presence of the pump pulse, and the homogeneous Lorentzian lines constituting the absorption band (dash-dotted lines).

50 mbar of nitrogen at 100 K, the nitrogen adsorbs to these O–D sites, resulting in a redshift of the peak due to the weak hydrogen bond to the adsorbate.[29] The resulting O–D groups will be further referred to as $OD\cdots N_2$ groups. Note the similarity between the LF O–D peak of $D_{0.19}Y$ due to the the $OD\cdots O_{latt}$ groups and that of the HF O–D of $NaD_{0.05}Y$ with adsorbed nitrogen, due to the $OD\cdots N_2$ groups.

In Fig. 2 the results of one-color pump–probe experiments are shown, from which the vibrational population lifetime can be obtained. It has been demonstrated that for these O–D vibrations the decay time of the pump-induced transmission increase can be interpreted straightforwardly as the vibrational lifetime T_1.[25] Upon adsorption of nitrogen the vibrational lifetime of the O–D groups drops from 171 to 48 ps, and this lifetime coincides remarkably well with the 44 ps lifetime of the $OD\cdots O_{latt}$ groups. We have shown recently[30] that this enhancement of the vibrational relaxation rate is neither due to desorption of the nitrogen (breaking of the weak hydrogen bond could be an efficient way for the O–D group to lose a considerable amount ($\approx$1000 cm^{-1}) of its excess vibrational energy), nor due to energy transfer into internal degrees of freedom of the adsorbate. The enhancement was attributed to an increased coupling of the O–D group to the lattice caused by the hydrogen bond, allowing for a more rapid energy dissipation (for details, see Ref. 30).

From Fig. 3 it is observed that, although the overall absorption line and the vibrational population lifetimes are similar for the two differently hydrogen-bonded O–D groups, the homogeneous linewidths are very different. Recording a transient spectrum at a delay between pump and probe of 20 ps, it is found that for the $OD\cdots O_{latt}$ groups, the pump pulse burns a hole in the absorption spectrum (see also Ref. 25), whereas, remarkably, for the $OD\cdots N_2$ groups the whole absorption band decreases in amplitude (both transient spectra were recorded at 100 K). The fact that a hole is burnt in the LF O–D absorption spectrum implies that this line is predominantly inhomogeneously broadened;[31] there is a distribution of vibrational frequencies for the O–D groups, and only those O–D groups can be excited that are resonant with the frequencies within the laser pump pulse.

In order to obtain the homogeneous linewidth, we have calculated the transient spectra. In these calculations the absorption band is deconvoluted into a sum of Lorentzians of full width at half maximum $\Gamma_{hom}^{0\rightarrow 1}$

$$A(\nu)=\sum_i \mathscr{L}_i(\nu), \quad \mathscr{L}_i(\nu)=a_i\frac{\Gamma_{hom}^{0\rightarrow 1}/\pi}{4(\nu-\nu_i)^2+(\Gamma_{hom}^{0\rightarrow 1})^2}, \tag{2}$$

where ν_i is the center frequency of the ith homogeneous Lorentzian line of amplitude a_i. The pump pulse excites a fraction f_i^0 of each Lorentzian, determined by the spectral overlap of the ith Lorentzian with the laser pump pulse as well as saturation effects (power broadening).[25] The excited spectrum then reads

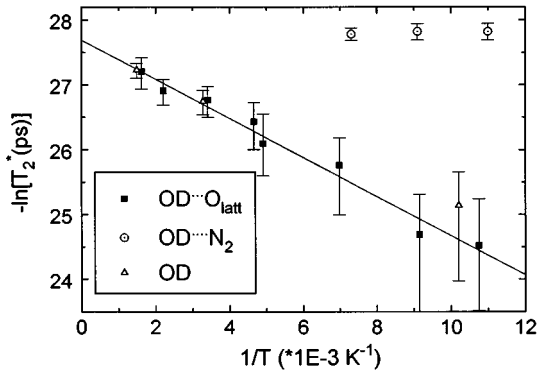

FIG. 4. Arrhenius plot of the pure dephasing time T_2^* vs temperature for the $OD\cdots O_{latt}$ and the $OD\cdots N_2$ hydroxyls. For both the LF OD $OD\cdots O_{latt}$ and the HF ''free'' OD groups, a least squares fit gives an activation energy of 200 ± 70 cm^{-1}. For the OD groups bonded to nitrogen, no temperature dependence is found.

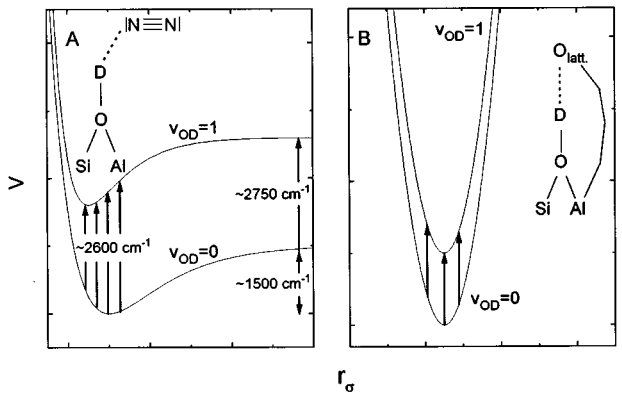

FIG. 5. Schematic r_σ potentials for the two differently hydrogen bonded systems: The lower curve is for the ν_s(O–D) in the ground state, upper curve in the first excited state. (A) For a hydrogen bond to an adsorbate, strongly anharmonic and dissociative. The H bond dissociation energy is ~ 1500 cm^{-1}, the transition frequency ~ 2600 cm^{-1} and ~ 2750 cm^{-1} with and without the H bond, respectively. After Ref. 34. (B) For a hydrogen bond to fixed lattice oxygen atoms.

$$A_{\rm exc}(\nu,t)=\sum_i\,[1-2f_i^0e^{(-t/T_1)}]\mathscr{L}_i(\nu), \tag{3}$$

where the initially excited fraction of excited oscillators, f_i^0, is assumed to decay exponentially with time-constant T_1. This spectrum (for $t=20$ ps) has to be convoluted with the laser probe spectrum to obtain the experimental excited spectrum. The results of this calculation are shown as dashed lines in Fig. 3. The corresponding FWHM homogeneous linewidth is 0.75 ± 0.4 cm^{-1} for the $OD\cdots O_{latt}$ groups and 13 ± 1 cm^{-1} for the $OD\cdots N_2$ system at 100 K. The insets of Fig. 3 show the absorption spectrum with and without pump pulse, along with an illustrative homogeneous Lorentzian of which the overall absorption line is built up. From the homogeneous linewidths and the independently measured T_1, we obtain pure dephasing times $T_2^*=20\pm 10$ ps for the $OD\cdots O_{latt}$ groups and 0.82 ± 0.1 ps for the $OD\cdots N_2$ system at 100 K.

The large difference in dephasing times T_2^* indicates the presence of different dephasing mechanisms for the two systems. This is confirmed by the difference in temperature dependence of the dephasing times T_2^* for the two systems shown as an Arrhenius plot in Fig. 4. For the $OD\cdots O_{latt}$ groups an apparent activation energy of 200 ± 70 cm^{-1} is observed. No temperature dependence is found for for the $OD\cdots N_2$ groups. The temperature dependence of the pure dephasing time of the HF O–D groups, situated in the large cages in the zeolite structure (not or only very weakly H bonded to the zeolite lattice) is also shown in Fig. 4. These data points coincide perfectly with those of the $OD\cdots O_{latt}$ groups, indicating that the same dephasing mechanism is operative for both the ''free'' HF O–D groups and the hydrogen-bonded LF $OD\cdots O_{latt}$ groups. This implies that, although it greatly affects the vibrational population lifetime, the hydrogen bond does not play an important role in the dephasing of the O–D stretch vibration for the $OD\cdots O_{latt}$ groups. However, the hydrogen bond does affect the overall absorption band: For the $OD\cdots O_{latt}$ groups, the broadening of the whole absorption line is due to a static distribution of hydrogen-bond strengths. This distribution of hydrogen-bond strengths is presumably due to the inhomogeneous distribution of Si and Al atoms throughout the zeolite lattice. It has been surmised[32] that the frequency of the O–H stretching vibration is sensitive to even the second Si/Al coordination shell. The conclusion that the inhomogeneous distribution is due to a distribution of different hydrogen bond strengths is substantiated by results of previous experiments which showed that the vibrational lifetime T_1 increases with increasing frequency within the absorption band,[33] due to the decrease of the hydrogen-bond strength.[28]

The large difference in the homogeneous linewidths for the $OD\cdots O_{latt}$ groups and the $OD\cdots N_2$ groups can be understood by considering the hydrogen-bond potentials for $v_{OD}=0$ and $v_{OD}=1$ for the two systems, which are schematically depicted in Fig. 5. By noting that the timescales associated with the high frequency the ν_s mode and the low-frequency ν_σ mode differ by over an order of magnitude, a vibrational Born–Oppenheimer approximation (also referred to as adiabatic approximation[5]) can be made. Thus, the slow motion of the r_σ coordinates is separated from the fast motion in the r_s coordinates. In this fashion the energies and wave functions of the system depend parametrically on the r_σ coordinate: The wave functions and eigenvalues can be calculated for a given value of r_σ, and by repeating this procedure for different r_σ, the variation of the energy of the system with this coordinate can be calculated. Thus the schematic potentials in Fig. 5 are obtained. In the presence of adsorbates, the potential is strongly anharmonic and dissociative. Furthermore, it is well known that the potentials for the ground and excited state are different[34]; the hydrogen bond is stronger for $v=1$ than for $v=0$, and hence the potential energy minimum is situated at smaller r_σ (O···X distance) for $v=1$.[34] Since D is determined by the *difference* between the $v=0$ and $v=1$ potentials, i.e., by a change in the hydrogen bond upon excitation of the O–D stretch vibration, D will be relatively large for this system. In contrast, for the

$OD\cdots O_{latt}$ the potential energy curve is dictated by *lattice* parameters; the $OD\cdots O_{latt}$ distance is determined not by the electrostatic interaction between the deuterium and the O_{latt}, but by the geometry of the zeolite lattice. The rigidity of the zeolite lattice strongly disfavors a change in the oxygen–oxygen distance. As a result the potential is non-dissociative, and very similar for the ground and excited state of the O–D vibration. As a result D will be relatively small, resulting in a narrow homogeneous absorption line. From the observation that the linewidths and the temperature dependence are the same for the free O–D groups and the $OD\cdots O_{latt}$ groups (Fig. 4), we deduce that the homogeneous linewidth broadening due to the interaction with the hydrogen bond is so small, that a different broadening mechanism dominates. The observation of the 200 ± 70 cm^{-1} activation energy is most likely due to the involvement of the 260 cm^{-1} zeolite (oxygen) lattice mode in the dephasing process (there are no other low-frequency modes between 100 and 300 cm^{-1}).[35] This 260 cm^{-1} mode involves the cooperative motion of zeolite oxygen atoms.[35] The observation of an apparent activation energy is in good agreement with the Shelby–Harris theory in the limit of slow modulation. Hence we conclude that, for the LF $OD\cdots O_{latt}$ groups, the coupling is properly accounted for by the Shelby–Harris theory, and that dephasing occurs by coupling to the 260 cm^{-1} zeolite (oxygen) lattice mode.

Another difference between the two differently hydrogen-bonded groups can be observed in the so-called hot-band absorption depicted in Fig. 6. From Fig. 6 it is clear that the hot-band absorption for the $OD\cdots O_{latt}$ groups has approximately the same width as the hole, whereas the hot band is much broader than the hole for the $OD\cdots N_2$ groups. These transient spectra were recorded at temperatures of 200 K and 100 K for the $OD\cdots O_{latt}$ and the $OD\cdots N_2$ groups, respectively.

The solid line through the data is a calculation for which each of the bleached Lorentzians constituting the absorption band are ν_{anh} anharmonically shifted from the original absorption band to form the hot band. In this calculation we assume that the $1\rightarrow 2$ transition frequency of an oscillator is correlated to the $0\rightarrow 1$ transition, in the sense that a transition corresponding to one of the Lorentzian lines on the red side of the absorption band will appear on the red side of the hot band: Each Lorentzian is exactly ν_{anh} cm^{-1} shifted. The excited spectrum then reads

$$A_{exc}(\nu,t)=\sum_i\,[1-2f_i^0e^{(-t/T_1)}]\mathscr{L}_i(\nu,\Gamma_{hom}^{0\rightarrow 1})$$

$$+\beta\sum_i\,f_i^0e^{(-t/T_1)}\mathscr{L}_i(\nu+\nu_{anh},\Gamma_{hom}^{1\rightarrow 2}). \qquad (4)$$

The first term corresponds to Eq. (3), and is due to the bleaching of the original absorption band, and the second term is the hot-band absorption. β is the ratio between the $1\rightarrow 2$ and the $0\rightarrow 1$ cross sections ($=2$ for a harmonic oscillator). This straightforward procedure describes the data for the $OD\cdots O_{latt}$ groups quite well, with $\Gamma_{hom}^{0\rightarrow 1}=2.2\pm 1$ cm^{-1}, $\nu_{anh}=90\pm 2$ cm^{-1} and $\beta=1.85$. In this calculation

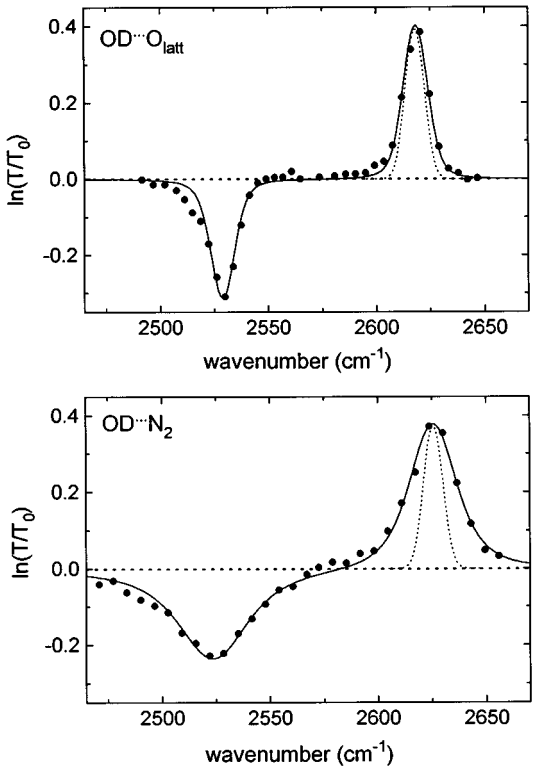

FIG. 6. Transient absorption spectra after excitation of the O–D stretch vibration for the $OD\cdots O_{latt}$ hydroxyls at 200 K (upper panel) and the $OD\cdots N_2$ hydroxyls at 100 K (lower panel). For the $OD\cdots O_{latt}$ the induced hot band absorption (negative $\ln[T(t)/T_0]$) associated with the $1\rightarrow 2$ transition has the same width as the hole (positive $\ln[T(t)/T_0]$) due to the bleaching of the $0\rightarrow 1$ transition. For the $OD\cdots N_2$ groups the hot band is significantly broader than the hole. Solid lines are calculations explained in the text, dotted lines denote the instrumental function (convolution of the 6 cm^{-1} laser pump and probe pulses).

$\Gamma_{hom}^{1\rightarrow 2}=2.7\pm 1$ cm^{-1}: $\Gamma_{hom}^{1\rightarrow 2}$ is additionally broadened by ≈ 0.5 cm^{-1} due to the 10 ps lifetime of the second excited state (see below). For the $OD\cdots N_2$ groups the width of the Lorentzians constituting the hot band, $\Gamma_{hom}^{1\rightarrow 2}$ has to be as large as 30 ± 4 cm^{-1} ($\Gamma_{hom}^{0\rightarrow 1}=13\pm 1$ cm^{-1}) to describe the experimental data, and $\beta=1.95$. The anharmonicity, $\nu_{anh}=100\pm 2$ cm^{-1} is significantly larger than that of the $OD\cdots O_{latt}$ groups. On the low-frequency side of both the hole and the hot band the calculations deviate slightly from the data, implying that the homogeneous linewidth varies slightly within the inhomogeneously broadened absorption band, as was found previously.[25] Hot bands with widths larger than the fundamental transition have been observed before in hydrogen-bonded systems.[19,20] In fact, in all of these experiments a similar ratio of $\Gamma_{hom}^{1\rightarrow 2}/\Gamma_{hom}^{0\rightarrow 1}$ of 2–3 was observed. In our calculations we assume that the $1\rightarrow 2$ transition center frequency of an oscillator is correlated to its $0\rightarrow 1$ transition. In principle this need not be the case; an ''inhomogeneous'' broadening mechanism for the $1\rightarrow 2$ transition could be the cause of the large width of the hot band. However, this is not very likely due to the fact that this broadening is not observed for the LF $OD\cdots O_{latt}$ and the HF O–D groups (without adsorbed nitrogen), and that the same

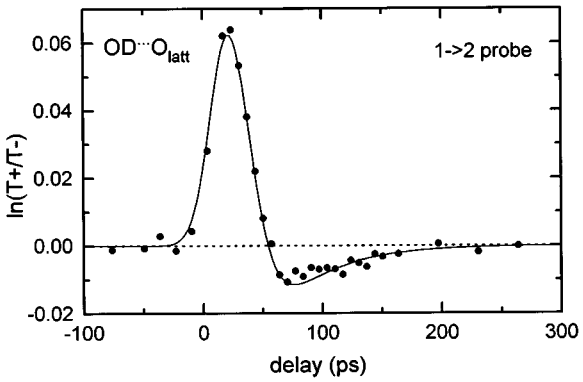

FIG. 7. Results of the pump–pump–probe experiments for the OD···O_{latt} groups. Transmission changes at the hot band frequency ($1\rightarrow2$ transition) due to the second pump pulse tuned to the $1\rightarrow2$ transition ($T+$ denotes transmission with, and $T-$ without second pump pulse) versus delay between the probe pulse and the pump pulses. The solid line is the result of calculations assuming decay from the second excited state $v=2$ to the ground state *via* $v=1$.

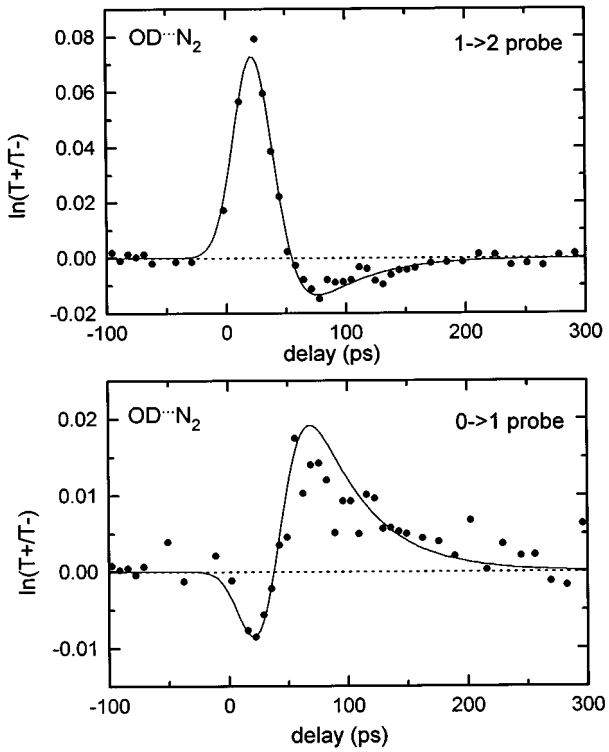

FIG. 8. Results of the pump–pump–probe experiments for the OD···N_2 groups. Upper panel: Transmission changes at the hot band frequency ($1\rightarrow2$ transition) due to the second pump pulse ($T+$ denotes transmission with, and $T-$ without second pump pulse). Lower panel: Transmission changes at the ground state absorption frequency ($0\rightarrow1$ transition) due to the second pump pulse. The solid lines are the results of calculations assuming decay from the second excited state $v=2$ to the ground state *via* $v=1$. Note that both data sets can be well accounted for by the same calculation.

relative width of the hot band is observed for methane absorption (see below). Therefore, the relatively large $\Gamma_{\text{hom}}^{1\rightarrow2}$ associated with the $1\rightarrow2$ transition for the OD···N_2 groups is caused by either a much shorter population lifetime $T_1^{2\rightarrow1}$ for the $v=2$ state, or a faster dephasing of the $1\rightarrow2$ transition (shorter $T_2^{*1\rightarrow2}$), since $\Gamma_{\text{hom}}^{1\rightarrow2}$ is determined by:[36] $2\pi\Gamma_{\text{hom}}^{1\rightarrow2} = (T_1^{1\rightarrow0})^{-1}+(T_1^{2\rightarrow1})^{-1} + (2T_2^{*1\rightarrow2})^{-1}$, where $T_1^{1\rightarrow0}$ and $T_1^{2\rightarrow1}$ are the population lifetimes of the first and second excited states, and $T_2^{*1\rightarrow2}$ is the pure dephasing time for the $1\rightarrow2$ transition. To check whether the $v=2$ population lifetime is the cause of the broadening, we measured this lifetime with pump–pump–probe experiments.[37]

For the pump–pump–probe experiments, the delay between the $(1\rightarrow2)$ pump and the $(0\rightarrow1)$ pump was fixed at 16 ps (the time at which the $v=1$ state population due to the $(0\rightarrow1)$ pump is maximal). The delay of the probe pulse, of the same frequency as one of the two pump pulses, is varied. In Fig. 7 the results of a pump-pump-probe experiments are shown for the OD···O_{latt} groups, with the probe frequency tuned to the $1\rightarrow2$ transition. In this figure, the transmission changes induced by the second pump pulse are plotted vs delay with respect to the first pump pulse. Clearly, the $(1\rightarrow2)$-pump excites a significant amount of oscillators to their second excited state, i.e., the hot-band absorption is bleached. With the $(0\rightarrow1)$ pump blocked, no signal was observed, confirming that the transmission changes due to the $(1\rightarrow2)$ pump result from up-pumping of the O–D oscillators to their second vibrationally excited state. The fact that after the transmission *increase* (bleaching), a transmission *decrease* is observed can be understood as follows: the probe pulse is monitoring the population difference between the $v=1$ and $v=2$ levels. If the oscillators in $v=2$ decay to $v=1$, then the long-time effect of the second pump pulse will be that there are more oscillators in $v=1$ than without the second pump pulse; the oscillators have been put ''on hold'' in the $v=2$ state for a time $T_1^{2\rightarrow1}$, so that the hot band $(1\rightarrow2$ absorption) will effectively live somewhat longer with than without the second pump pulse. The experimentally observed signals were calculated by numerically solving the appropriate set of coupled rate equations for a three level system, rendering the time-dependent population distribution. Subsequently, the transmission of the probe pulse is evaluated. Input parameters are pulse (intensities, duration and shape) and sample (absorption cross sections, oscillator density and sample length) characteristics. The result using a lifetime $T_1^{2\rightarrow1}$ of 10 ps is shown in Fig. 7 as a solid line. Although this lifetime is shorter than the duration of our pulses, we can deduce that the error in this value is not larger than 5 ps from both the amplitude and width of the signal. Decay from $v=2$ directly to the ground state has been observed in this type of experiment,[37] but is clearly not occurring in this system, since in the case of direct relaxation, the signal would have a distinctly different shape:[37] In case of direct decay to the ground state, the overshoot of the transmission decrease after the bleaching of the hot band is not observed. In Fig. 8 the results are shown for the OD···N_2 groups, with the probe tuned to the $1\rightarrow2$ transition, and the $0\rightarrow1$ transition, respectively. The results of the same calculations with exactly the same input parameters were used to describe both data sets, and a again a lifetime $T_1^{2\rightarrow1}$ of 10 ps was found. Obviously, this value is too large to account for the observed width of the hot band of 30 cm^{-1}. We therefore

conclude that the observation of the large hot-band width must be due to a faster pure dephasing for the $1\rightarrow 2$ transition ($T_2^{*1\rightarrow 2} = 0.35\pm 0.05$ ps) compared to that of the $0\rightarrow 1$ ($T_2^{*0\rightarrow 1} = 0.82\pm 0.1$ ps) transition for the OD$\cdots$N$_2$ groups.

B. Coupling mechanism for hydrogen-bond induced dephasing

We have shown in the previous section that for the OD$\cdots$O$_{\text{latt}}$ groups the dephasing mechanism can be described by the Shelby–Harris coupling model. However, in that case the homogeneous linewidth is not caused by coupling to the hydrogen-bond mode. In contrast, for the O–D groups with adsorbates coupling to the hydrogen bond is responsible for the observed linewidths. In this section we will investigate the coupling mechanism for this system.

The temperature dependence of the homogeneous linewidth of the OD$\cdots$N$_2$ groups does not provide conclusive information on the type of coupling between the high-frequency and the hydrogen-bond stretching modes. The absence of a significant temperature dependence (the same observation was made for other adsorbates) can be explained by both the Shelby–Harris and the Robertson–Yarwood model. The temperature-activated behavior predicted by the Shelby–Harris model is valid only in the low-temperature (slow modulation) limit and therefore the absence of temperature dependence might be due to the possibility that for this system the modulation is intermediate or fast. As far as the Robertson–Yarwood model is concerned, it does not predict a significant dependence of the linewidth on temperature. It is clear, however, that in the Robertson–Yarwood type of coupling the temperature dependence can be very complicated: Increasing the temperature will lead to an increase of the spectral distribution D due to an increase in the rms displacement of r_σ, $\langle r_\sigma^2\rangle^{1/2}$. Furthermore, this theory would also predict a temperature dependent τ_c if the low-frequency mode were treated quantum mechanically:[38,39] In a quantum-mechanical description, the stochastic modulation of the high-frequency mode is a result of ongoing energy exchange between the quantum levels of the hydrogen bond and the bath. With increasing temperature the rate of exchange will increase leading to a decrease of τ_c. On the other hand, with increasing temperature the hydrogen bond stretching frequency may decrease due to the strong anharmonicity of the hydrogen bond, leading to an increase of τ_c. In conclusion, a change in temperature can have very different, counteracting, effects on the linewidth. Hence, it is clear that temperature is not a suitable parameter to investigate the nature of the coupling between the high-frequency and the hydrogen-bond mode.

It is interesting to note that the theoretical models of Shelby–Harris and Robertson–Yarwood make diametrically opposed predictions concerning the linewidth upon changing the *frequency* of the ν_σ(XH$\cdots$Y) hydrogen bond stretch vibration. The Shelby–Harris model predicts the following: An increase of the ν_σ(XH$\cdots$Y) frequency will result in a slower exchange with the bath, and hence a slower modulation (larger τ_c) of the high-frequency vibration. The absence of a temperature dependence for the homogeneous linewidth of the O–D groups with adsorbates implies that the frequency modulation of the high-frequency O–D mode does not occur in the regime of slow modulation. In the regime of intermediate or fast modulation, a slower modulation will result in a broadening of the line, since less motional narrowing will occur. In contrast, the Robertson and Yarwood model predicts a narrowing of the line, since in this model the coordinate r_σ determines the dephasing directly and $r_\sigma(t)$ will fluctuate more rapidly with increasing ν_σ(XH$\cdots$Y) frequency. The faster modulation will lead to more motional narrowing, since $\tau_c=\gamma/\nu_\sigma^2$, and therefore the absorption linewidth will become smaller. Hence it is clear that the decisive test between the two theoretical models is a change of the ν_σ hydrogen bond stretching frequency. By adsorbing a molecule different from nitrogen, a change in ν_σ can easily be achieved. For a meaningful comparison between the theories, a requirement is that the shape of the $v=0$ and $v=1$ potentials (determining the spectral distribution D) and thus the adsorption energy remains the same. A good candidate is methane. Methane produces the same shift of the O–D stretching frequency (and a very similar absorption line)[30] but has only half the mass of nitrogen, and hence ν_σ will increase by approximately a factor of $\sqrt{2}$, since the reduced mass of this vibration will be determined predominantly by the mass of the adsorbate. As shown in Fig. 9, the homogeneous linewidth decreases significantly from 13 ± 1 cm^{-1} for O–D$\cdots$N$_2$ to 8 ± 1 cm^{-1} for O–D$\cdots$CH$_4$, demonstrating the validity of the Robertson–Yarwood model for this system. The vibrational population lifetime for the O–D$\cdots$CH$_4$ groups was the same as for the O–D$\cdots$N$_2$ groups ($\sim$15 ps) and therefore does not contribute to the width of the homogeneous line. Nitrogen and methane were both adsorbed to deuterated mordenite zeolite (methane adsorbs poorly to Y zeolite). For the calculation for nitrogen adsorption, shown as a solid line in Fig. 9, exactly the same parameters were employed as those describing adsorption to Y zeolite: a homogeneous linewidth of 13 cm^{-1}, an excited state linewidth of 30 cm^{-1}, and $\beta=1.95$. Only the anharmonicity was found to be different (120 ± 2 cm^{-1} for Mordenite, as opposed to 100 ± 2 cm^{-1} for Y-zeolite). This means that, despite the different contributions from inhomogeneous broadening, the homogeneous linewidth is independent of zeolite structure. For methane the calculations show that $\Gamma_{\text{hom}}^{0\rightarrow 1} = 8\pm 1$ cm^{-1}, $\Gamma_{\text{hom}}^{1\rightarrow 2} = 20\pm 3$ cm^{-1}, $\nu_{\text{anh}} = 115\pm 2$ and $\beta=2.0$; Again, the hot band is much broader than the fundamental transition as also observed for O–D$\cdots$N$_2$. In Fig. 10 the transient spectra resulting from adsorption of xenon and carbon monoxide are shown. For xenon adsorption, almost the whole absorption band is bleached, indicating that the homogeneous linewidth is very large. The solid line shows the absorption spectrum as recorded by the laser probe pulses. Obviously, this absorption line is almost completely homogeneously broadened. The spike at exactly the pump frequency is due to (LF) O–D groups to which no xenon is adsorbed. These free O–D groups have a very narrow homogeneous linewidth. The decreased transmission on the red side is due to excited state absorption. For the O–D groups with carbon monoxide ad-

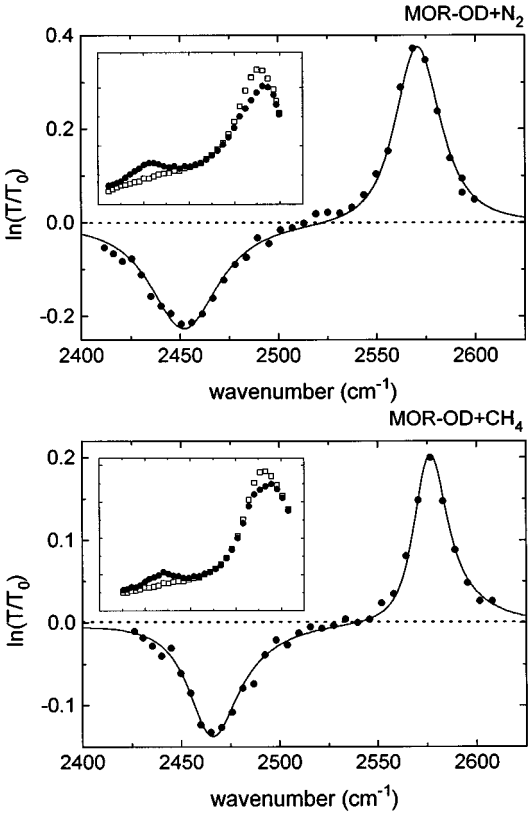

FIG. 9. Transient absorption spectra after excitation of the O–D stretch vibration for the OD···N_2 hydroxyls at 100 K (upper panel) and the OD···CH_4 hydroxyls at 120 K (lower panel). The O–D groups are situated in zeolite Mordenite. Insets show the absorption spectra with (●) and without (□) the pump pulse, as recorded by the laser probe pulses. Although the overall absorption spectra are very similar, the bleaching (and therefore the homogeneous linewidth) is significantly narrower for the OD···CH_4 hydroxyls. Lines are calculations explained in the text.

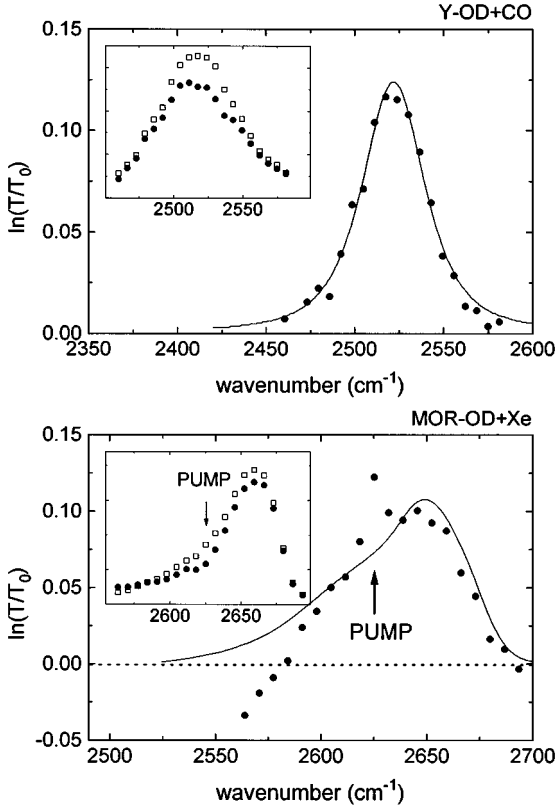

FIG. 10. Transient absorption spectra after excitation of the O–D stretch vibration for the OD···Xe hydroxyls in D-Mordenite at 170 K (upper panel) and the OD···CO hydroxyls (lower panel) in $NaD_{0.05}Y$ at 100 K. Insets show the absorption spectra with (●) and without (□) the pump pulse, as recorded by the laser probe pulses. For xenon adsorption the small spike at the pump frequency is due to O–D groups without adsorbed Xe (with a very narrow homogeneous line), and on the red side excited state absorption sets in. Lines are calculations explained in the text.

sorbed, a homogeneous linewidth of 22 ± 2 cm^{-1} is observed. The results of the experiments are summarized in Table I.

The Robertson–Yarwood expression for τ_c provides a quantitatively correct description of the data for all adsorbates. Assuming a damping parameter γ of 50 cm^{-1} in accordance with Refs. 15, 13, and 14, and a ν_σ(OD···X) frequency of 100 cm^{-1} for X=N_2,[40] we find that a value of 46 cm^{-1} for D is required to account for the observed hole of 14 cm^{-1} (implying $D\tau_c = 0.23$, i.e., the modulation is in the intermediate modulation regime and motional narrowing is important in the description of the linewidth). We take this set as a reference to calculate the linewidths for the other adsorbates. We approximate $V(r_\sigma)$ by a Morse potential: $V(r_\sigma)=E_{\text{ads}}(1-e^{-a(r_\sigma/r_0)})$, where E_{ads} is the absorption energy, and hence dissociation energy, and a determines the degree of anharmonicity of the hydrogen-bond potential. This anharmonicity parameter a is determined from the $0\rightarrow1$ transition frequency and the adsorption energy. If the degree of anharmonicity of the (OD···X) potential remains the same for the different adsorbates, then for the other adsorbates the ν_σ(OD···X) frequency is readily calculated as a function of adsorption energy E_{ads} and adsorbate mass M_{ads} (viz. the reduced mass of this vibration)

$$\nu_\sigma(E_{\text{ads}},M_{\text{ads}})=\nu_\sigma^{N_2}\frac{M_{N_2}\left[2\sqrt{2}M_{\text{ads}}\sqrt{\frac{E_{\text{ads}}}{M_{\text{ads}}}}\pi-ah\right]}{M_{\text{ads}}\left[2\sqrt{2}M_{N_2}\sqrt{\frac{E_{\text{ads}}^{N_2}}{M_{N_2}}}\pi-ah\right]}, \tag{5}$$

with h Planck's constant. If γ is independent of adsorbate, we obtain τ_c, also shown in Table I. We assume that D, determined by the difference between the ground-state and excited-state potential, scales linearly with the heat of adsorption. The calculated linewidths resulting from numerically solving the integral of Eq. (1) are shown in Table I. The agreement with the data is excellent, and it should be noted that the results depend only weakly on the assumed reference values for γ and ν_σ for nitrogen, as long as these values reproduce the observed linewidth of 13 cm^{-1} for nitrogen.

It is clear that for the O–D···C_4 groups the small homogeneous linewidth as compared to the O–D···N_2 is due to the increased effect of motional narrowing: the frequency of the ν_σ mode is increased, whereas D remains practically unal-

TABLE I. Characteristics and effects of different adsorbates on zeolites Y and Mordenite: The shift from the original O–D stretch frequency by the adsorbate $\Delta\tilde{\nu}_{OD}$, the width of this line Γ_{OD}, the heat of adsorption E_{ads}, the experimentally observed homogeneous linewidth Γ_{hom}^{exp}, calculated spectral distributions D, calculated correlation times τ_c, and the calculated homogeneous linewidth Γ_{hom}^{calc}. All widths are FWHM and errors denote 2σ.

Adsorbate	Zeolite	M_{ads} (a.m.u.)	$\Delta\tilde{\nu}_{OD}$ (cm^{-1})	Γ_{OD} (cm^{-1})	E_{ads}[a] (eV)	Γ_{hom}^{exp} (cm^{-1})	D (cm^{-1})	τ_c (s)	$D\tau_c$	Γ_{hom}^{calc} (cm^{-1})
N_2	D-Mor	32	65 ($\pm$3)	61 ($\pm$3)	0.16	13 ($\pm$1)	51	1.66×10^{-13}	0.25	13 (Ref.)
	D-Y	32	60 ($\pm$3)	42 ($\pm$3)	0.16	13 ($\pm$1)	51	1.66×10^{-13}	0.25	13 (Ref.)
CH_4	D-Mor	16	60 ($\pm$3)	50 ($\pm$3)	0.15	8 ($\pm$1)	47.5	1.14×10^{-13}	0.16	7.5
CO	D-Y	32	168 ($\pm$3)	65 ($\pm$3)	0.23	22 ($\pm$2)	73	1.12×10^{-13}	0.24	19.5
Xe	D-Mor	131.3	45($\pm$6)	30 ($\pm$4)	0.12	28 ($\pm$4)	38	11.8×10^{-13}	1.34	29.8

[a]Heats of adsorption for CO and N_2 obtained from Ref. 43, others are estimated from $\Delta\tilde{\nu}_{OD}$ (see Ref. 40).

tered. For xenon the ν_σ(OD···Xe) frequency is relatively low due to the high mass of xenon. Hence τ_c is relatively large, and in this case *less* motional narrowing will occur. Indeed, despite the smaller adsorption energy and hence smaller D, a very broad homogeneous line is observed. For CO, its relatively strong adsorption results in both a large D and a small τ_c compared to nitrogen. The correlation time is very similar to that of methane: although the relatively strong hydrogen bond will lead to an increase of the frequency of the ν_σ mode, the higher reduced mass of the O–D···CO compared to O–D···CH_4 will lower this frequency.

In general, the anharmonic coupling term can be expanded as a power series of the normal coordinates r_s and r_σ as:

$$V_{anh}(r_s,r_\sigma)=\mathcal{F}(r_\sigma)(ar_s+br_s^2+cr_s^3+\ \ldots). \tag{6}$$

Since for the O–D groups with adsorbates our observations can be well accounted for by the Robertson–Yarwood model, this means that the coupling is first order in r_σ Hence, it must be that $\mathcal{F}(r_\sigma)\propto r_\sigma$. What is equally interesting, is the fact that the hot band is broader than the hole, i.e., $\Gamma_{hom}^{1\rightarrow2}$ is larger than $\Gamma_{hom}^{0\rightarrow1}$. This implies that *third*-order coupling terms in r_s are important in the anharmonic coupling term. This can be understood as follows: Consider a potential with negligible anharmonicity in the O–D distance r_s, i.e., the potential $V(r_s;r_\sigma)$ which depends parametrically on the hydrogen-bond coordinate r_σ in the Born–Oppenheimer approximation. Then for a given value of r_σ, the potential $V(r_s;r_\sigma)$ is the sum of a term quadratic in r_s and V_{anh}: $V(r_s;r_\sigma)=\alpha r_s^2+V_{anh}(r_s,r_\sigma)$. If only linear terms in r_s in Eq. (6) contribute to the anharmonic coupling term $V_{anh}(r_s,r_\sigma)$, then the $V(r_s;r_\sigma)$ potential is still completely harmonic, the spacing between the energy levels is constant and independent of r_σ. This means that the transition frequencies between the energy levels are the same and that these cannot be broadened due to the hydrogen bond. Another way of understanding this is that, in case only linear terms in r_s contribute to V_{anh}, the hydrogen bond potentials $V(r_\sigma)$ for the ground state ($v_{OD}=0$) and the excited states (v_{OD}=1, 2, etc.) are exactly the same. Indeed, none of the transitions will be broadened, since the spectral distribution D is determined by the *difference* between the potentials. In this case the absorption line as well as the hot band would be infinitely narrow. If the r_s^2 terms become important, the $0\rightarrow1$ and the $1\rightarrow2$ transitions will both be equally broadened.[36,41,42] In this case, a change in r_σ induces a difference between the ($v_{OD}=0$) and ($v_{OD}=1$) hydrogen-bond potentials, that is equal to the difference between the ($v_{OD}=1$) and ($v_{OD}=2$) potentials: The hole and the hot band will both have the same, non-zero width. It is only when third- or higher-order terms become significant that the width of the $0\rightarrow1$ will be different from that of the $1\rightarrow2$. In this case, the difference between the $V(r_\sigma)$ hydrogen bond potentials for v_{OD}=1 and v_{OD}=2 will be larger than the difference between v_{OD}=0 and v_{OD}=1 potentials. This situation is schematically depicted in Fig. 11. The spectral distribution

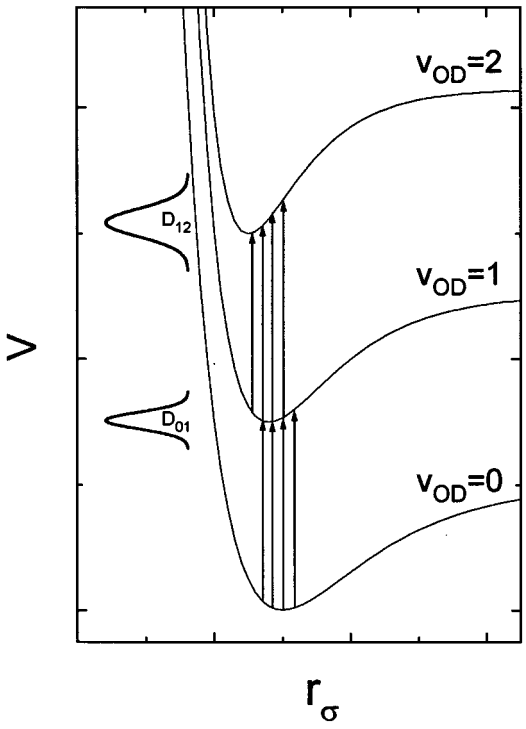

FIG. 11. Schematic r_σ potentials for the hydrogen bonded OD··· Adsorbate system for the ν_s(O–D) in the ground, first and second excited state. The $1\rightarrow2$ transition is broadened compared to the $0\rightarrow1$ transition, indicating third- or higher-order terms in r_s contribute significantly to the anharmonic coupling term V_{anh}.

associated with the $1\rightarrow 2$ transition $D_{1\rightarrow 2}$ is broader than that of the $0\rightarrow 1$ transition $D_{0\rightarrow 1}$, accounting for the broader hot band. Hence it is concluded that the coupling between the ν_s and the ν_σ mode is *linear* in the hydrogen bond coordinate r_σ, and that third- or higher-order terms in r_s contribute significantly to the anharmonic coupling term.

For the $OD\cdots O_{latt}$ groups, for which the hole and the hot band have the same width, it is clear that anharmonic coupling terms of higher than second order in r_s do not significantly contribute. This is in agreement with the Shelby–Harris model that states that the predominant terms are of second-order in both the low- and high- frequency coordinate. These different coupling terms for the $OD\cdots O_{latt}$ and the $OD\cdots N_2$ groups also explain the different anharmonicities of 92 and 100 cm^{-1}, respectively. The third-order r_s term in the V_{anh} of the $OD\cdots N_2$ groups will lead to an increase of the anharmonicity of the effective potential in r_s of the O–D stretching vibration, whereas the second-order terms for the $OD\cdots O_{latt}$ groups will not.

V. SUMMARY AND CONCLUSIONS

We have shown that the effect of a hydrogen bond on the vibrational line shape depends critically on the nature of the hydrogen bond. If the potential energy as a function of the hydrogen-bond coordinate is solely determined by the electrostatic interaction between the hydrogen atom and the hydrogen bonding partner, this will result in broad homogeneous lines, as observed for O–D groups to which simple molecules are adsorbed. In the case that the structure is rigid, however, it is not the hydrogen bond that determines the homogeneous linewidth, and we observe that the linewidth is determined by coupling to a ~ 200 cm^{-1} lattice mode. If the homogeneous linewidth is determined by the hydrogen bond, (in case of the adsorbates) we find that variation of the adsorbates allows us to investigate the coupling between the high-frequency ν_s (O–D) stretching mode and the low-frequency ν_σ ($OD\cdots X$) stretching mode. From the variation of adsorbate, we find strong evidence that this coupling is linear in the r_σ coordinate. From the fact that the $1\rightarrow 2$ transition is broadened compared to the $0\rightarrow 1$ transition, we deduce that third- or higher-order terms in r_s contribute significantly to the coupling term.

ACKNOWLEDGMENTS

We kindly acknowledge Sander Woutersen for helpful discussions and Erik Kossen and Richard Schaafsma for technical assistance. The work described in this paper is part of the research program of the Stichting Fundamenteel Onderzoek van de Materie (Foundation for Fundamental Research on Matter) and was made possible by financial support from the Nederlandse Organisatie voor Wetenschappelijk Onderzoek (Netherlands Organization for the Advancement of Research).

[1] D.W. Oxtoby, Adv. Chem. Phys. **40**, 1 (1979).
[2] R. Kubo, J. Phys. Soc. Jpn. **9**, 935 (1954).
[3] P.W. Anderson, J. Phys. Soc. Jpn. **9**, 316 (1954).
[4] R.M. Shelby, C.B. Harris, and P.A. Cornelius, J. Chem. Phys. **70**, 34 (1979); S. Marks, P.A. Cornelius, and C.B. Harris, *ibid.* **73**, 3069 (1980).
[5] Y. Marechal and A. Witkowski, J. Chem. Phys. **48**, 3697 (1968).
[6] S. Bratos, J. Chem. Phys. **63**, 3499 (1975).
[7] J. Yarwood and G.N. Robertson, Nature **257**, 41 (1975); G.N. Robertson and J. Yarwood, Chem. Phys. **32**, 267 (1978).
[8] H. Abramczyk, Chem. Phys. **144**, 319 (1990).
[9] J.P. Hawranek and M.A. Broda, Chem. Phys. Lett. **98**, 373 (1983).
[10] U.P. Agarwal, R.S. Green, and J. Yarwood, Chem. Phys. **74**, 35 (1983).
[11] J. Yarwood, R. Ackroyd, and G.N. Robertson, Chem. Phys. Lett. **78**, 614 (1981).
[12] M.I. Cabaço, M. Besnard, and Y. Yarwood, Mol. Phys. **75**, 139 (1992).
[13] B. Czarnik-Matusewicz and J.P. Hawranek, Spectrochim. Acta **43A**, 791 (1987).
[14] K. Tokhadze, N. Dubovna, Z. Mielke, M. Wierzejewska-Hnat, and H. Ratajczak, Chem. Phys. Lett. **202**, 87 (1993).
[15] J. Yarwood, R. Ackroyd, and G.N. Robertson, Chem. Phys. **32**, 283 (1978).
[16] J.M. Thomas, Sci. Am. **266** (IV), 82 (1992).
[17] M. Bonn, M.J.P. Brugmans, H.J. Bakker, A.W. Kleyn, and R.A. van Santen, *Proceedings of the 11th International Zeolite Conference* (Seoul, Korea) (to be published).
[18] C.P. Slichter, *Principles of Magnetic Resonance*, 3rd ed. (Springer-Verlag, Berlin, 1989).
[19] H. Graener, T.Q. Ye, and A. Laubereau, Phys. Rev. B **41**, 2597 (1990).
[20] H. Graener, G. Seifert, and A. Laubereau, Phys. Rev. Lett. **66**, 2092 (1991).
[21] D. Zimdars, A. Tokmakoff, S. Chen, S.R. Greenfield, and M.D. Fayer, Phys. Rev. Lett. **70**, 2718 (1993).
[22] R. Janoschek, E.G. Wiedemann, and G. Zundel, J. Chem. Soc. Faraday Trans. 2 **69**, 505 (1973).
[23] D. Borgis, G. Tarjus, and H. Azzouz, J. Chem. Phys. **97**, 1390 (1992).
[24] S.J. Klippenstein and J.T. Hynes, J. Phys. Chem. **95**, 4651 (1991).
[25] M.J.P. Brugmans, H.J. Bakker, and A. Lagendijk, J. Chem. Phys. **104**, 64 (1996).
[26] M. Bonn, M.J.P. Brugmans, A.W. Kleyn, and R.A. van Santen, J. Chem. Phys. **102**, 2181 (1995).
[27] M. Czjzek, H. Jobic, A.N. Fitch, and T. Vogt, J. Phys. Chem. **96**, 1535 (1992).
[28] M.J.P. Brugmans, A.W. Kleyn, A. Lagendijk, W.P.J.H. Jacobs, and R.A. van Santen, Chem. Phys. Lett. **217**, 117 (1994).
[29] F. Wakabayashi, J. Kondo, W. Akihide, K. Domen, and C. Hirose, J. Phys. Chem. **97**, 10761 (1994).
[30] M. Bonn, M.J.P. Brugmans, A.W. Kleyn, and R.A. van Santen, Chem. Phys. Lett. **233**, 309 (1995).
[31] A.E. Siegman, *Lasers* (University Science Books, Mill Valley, 1986).
[32] J. Dwyer, in *Innovation in Zeolite Material Science*, edited by P.J. Grobet *et al.* (Elsevier, Amsterdam, 1988), p. 333.
[33] M. Bonn, M.J.P. Brugmans, A.W. Kleyn, R.A. van Santen, and A. Lagendijk, Stud. Surf. Sci. Cat. **84**, 493 (1994).
[34] C. Sandorfy, in *Hydrogen Bonds*, edited by P. Schuster (Springer-Verlag, Berlin, 1984), p. 41.
[35] N.D. Baker, G.A. Ozin, and J. Godber, Catal. Rev. Sci. Eng. **27**, 591 (1985).
[36] D.W. Oxtoby and S.A. Ryce, Chem. Phys. Lett. **42**, 1 (1976).
[37] M. Bonn, M.J.P. Brugmans, and H.J. Bakker, Chem. Phys. Lett. **249**, 81 (1996).
[38] B. Boulil, O. Henri-Rousseau, and P. Blaise, Chem. Phys. **126**, 263 (1988).
[39] H. Abramczyk, Chem. Phys. **144**, 305 (1990).
[40] D. Hadži and S. Bratos, in *The Hydrogen Bond*, edited by P. Schuster, G. Zundel, and C. Sandorfy (North-Holland, Amsterdam, 1976), Vol 2, p. 565.
[41] P.A. Madden and R.M. Lynden-Bell, Chem. Phys. Lett. **38**, 163 (1976).
[42] M.R. Battaglia and P.A. Madden, Mol. Phys. **36**, 1601 (1978).
[43] K.M. Neyman, P. Strodel, S.P. Ruzakin, N. Schlensog, H. Knözinger, and N. Rösch, Cat. Lett. **31**, 273 (1995).